

Condensation of Plasmids Enhanced by Z-DNA Conformation of d(CG)_n Inserts[†]

Chenglie Ma, Lei Sun,[‡] and Victor A. Bloomfield*

Department of Biochemistry, University of Minnesota, St. Paul, Minnesota 55108

Received September 22, 1994; Revised Manuscript Received December 30, 1994[®]

ABSTRACT: DNA molecules collapse into compact structures in the presence of multivalent cations. To probe the possible importance of supercoiling and conformational effects, pUC18 plasmids (2686 bp) were modified by inserting 12-bp and 20-bp alternating d(CG)_n sequences, which are capable of converting to a left-handed Z-conformation under appropriate conditions, into the polycloning region. Condensation was induced by rapid addition of hexaammine cobalt(III) [Co(NH₃)₆³⁺] and monitored by laser light scattering and electron microscopy. Light scattering shows that plasmids with longer d(CG)_n inserts condense more extensively at natural superhelical densities. Electron microscopy indicates that the morphological distribution of condensed d(CG)_n-containing plasmids changes as a function of Co(NH₃)₆³⁺ concentration. At lower Co(NH₃)₆³⁺ concentration, the proportion of rods is higher, and at higher Co(NH₃)₆³⁺ concentration, most of the condensates have the form of toroids. In addition, the inner radii of the toroids are much smaller relative to condensed pUC18 under the same conditions. Enzymatic analysis and chemical probing show that the d(CG)_n inserts in naturally supercoiled plasmids have extensively converted from B-form to Z-form in the presence of Co(NH₃)₆³⁺ at the upper range of concentrations under which condensation occurs. To determine whether the enhanced condensation of d(CG)_n-containing plasmids results from the change of superhelical density due to the B–Z transition, we treated wild-type pUC18 molecules with topoisomerase I and varying amounts of ethidium bromide to generate a range of supercoil densities. Light scattering indicates that supercoiling did not affect the condensation process. Plasmids containing two inserts separated by 0.6 kb condense more extensively than those containing just one insert. We conclude that the B–Z transition of d(CG)_n inserts enhances DNA condensation, perhaps through the higher flexibility of secondary structure around the d(CG)_n insert region, greater exposure of bases to solvent in the Z-form, or the alteration of a larger region of flanking DNA.

DNA is tightly packaged in its biological milieu within cells and viruses. *In vitro*, plasmids and other DNA molecules condense into compact structures in the presence of multivalent cations. Condensation can be induced in aqueous solution by cations of charge 3+ or more (Arscott *et al.*, 1990; Chatteraj *et al.*, 1978; Gosule & Schellman, 1976; Plum *et al.*, 1990; Widom & Baldwin, 1980, 1983; Wilson & Bloomfield, 1979), such as hexaammine cobalt(III), spermidine(III), and spermine(IV). If carefully condensed from very dilute solution, DNA has a well-ordered morphology, generally toroidal but occasionally rodlike. The mechanism of *in vitro* DNA condensation by multivalent cations is still unclear despite much experimental and theoretical work. In this paper we explore the role of localized Z-DNA formation in condensation of plasmids.

In order for DNA or any other polymer to collapse, attractive interactions must outweigh repulsive ones. The repulsive contributions include entropy loss, bending or kinking energy, electrostatic repulsion (Marquet & Houssier, 1991; Riemer & Bloomfield, 1978), and hydration structure (Rau *et al.*, 1984). The list of postulated attractive interactions includes cross-linking (Schellman & Parthasarathy, 1984) or bending (Marquet *et al.*, 1985; Porschke, 1984) by bound ligands, polarization of fluctuating counterion clouds

(Marquet & Houssier, 1991; Oosawa, 1971; Riemer & Bloomfield, 1978) or water structure (Rau & Parsegian, 1984, 1992) near the DNA surface, and intrinsic local curvature or buckling of DNA when a critical degree of charge neutralization is achieved (Manning, 1978, 1980, 1981). At least as initially formulated, these interactions are all general ones, depending only on the general structural and polyelectrolyte properties of DNA and with no specific dependence on base composition or sequence.

However, there is increasing evidence that sequence-dependent distortions of the B-DNA double helix may play an important role in DNA condensation. In particular, alternating purine–pyrimidine sequences that can form Z-DNA under appropriate conditions also have a tendency to aggregate or condense under the same conditions (Castleman & Erlanger, 1983; Chaires & Norcum, 1988; Revet *et al.*, 1983; Thomas *et al.*, 1985). Furthermore, the same cations—spermidine, spermine, and Co(NH₃)₆³⁺—that cause DNA condensation in dilute aqueous solution also are effective in inducing the B–Z transition in poly(dG–dC) and poly(dG–m⁵dC) (Behe & Felsenfeld, 1981).

Despite the strong circumstantial connection between DNA condensation and the formation of Z-DNA, the fact remains that most random DNA sequences will condense although they cannot adopt the Z-conformation. This has led us to consider the possibility that localized conformational transitions induced by multivalent cations are sufficient to provoke condensation. d(CG)_n sequences inserted into naturally negative supercoiled plasmids can form Z-DNA while the rest of the plasmid DNA remains in the B conformation

[†] This research was supported in part by NIH Research Grant GM28093. L.S. was supported in part by NIH Research Grant GM40775 to Professor James Fuchs.

[‡] Present address: Cutaneous Biology Research Center, Harvard Medical School, Charlestown, MA 02129.

[®] Abstract published in *Advance ACS Abstracts*, February 15, 1995.

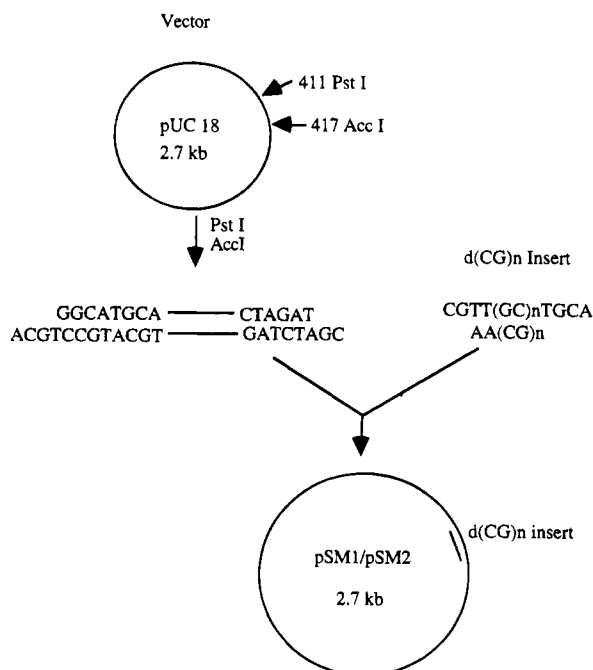


FIGURE 1: Schematic diagram for construction of plasmids pSM1 and pSM2, obtained by inserting oligonucleotides d(CG)₆ and d(CG)₁₀, respectively, into the parental plasmid pUC18 at the *Pst*I and *Acc*I sites.

(Peck *et al.*, 1982; Singleton *et al.*, 1982). The free energy of negative supercoiling is a powerful force for stabilization of Z-DNA.

We therefore sought to test the relations between DNA condensation, localized Z-conformation, and supercoiling by inserting 12 and 20 base pairs of alternating d(CG)_n sequences into the polycloning region of pUC18 (2686 bp) and determining the effects of added Co(NH₃)₆³⁺. To determine whether the enhanced condensation of d(CG)_n-containing plasmids results from the change of supercoiling due to the B–Z transition, rather than the formation of Z-DNA *per se*, we treated wild-type pUC18 molecules with topoisomerase I and varying amounts of ethidium bromide to generate a range of supercoil densities. We monitored DNA condensation by changes in light scattering intensity and determined the morphological forms of condensates by electron microscopy. In order to study the conformations of the small d(CG)_n inserts, we used S1 nuclease susceptibility, chemical probing, and restriction enzyme digestion. We found that the B–Z transition of d(CG)_n inserts enhances DNA condensation, the effect being stronger for the longer inserts, but that changes in supercoiling without Z-DNA formation did not affect condensation.

MATERIALS AND METHODS

Chemicals and Enzymes. Agarose was purchased from Pharmacia (Piscataway, NJ). Highly purified cobalt hexamine chloride was purchased from Kodak (Rochester, NY). Diethyl pyrocarbonate (DEPC) and piperidine were purchased from Sigma (St. Louis, MO) and stored at 4 °C. DNA ladder (1 kb), topoisomerase I, S1 nuclease, T4 DNA ligase, and calf intestinal phosphatase (CIP) were obtained from Gibco-BRL (Gaithersburg, MD). All restriction endonucleases were purchased from New England Biolabs (Beverly, MA).

Construction of d(CG)_n-Containing Plasmids. The DNAs studied were plasmid pUC18 and its recombinant plasmids.

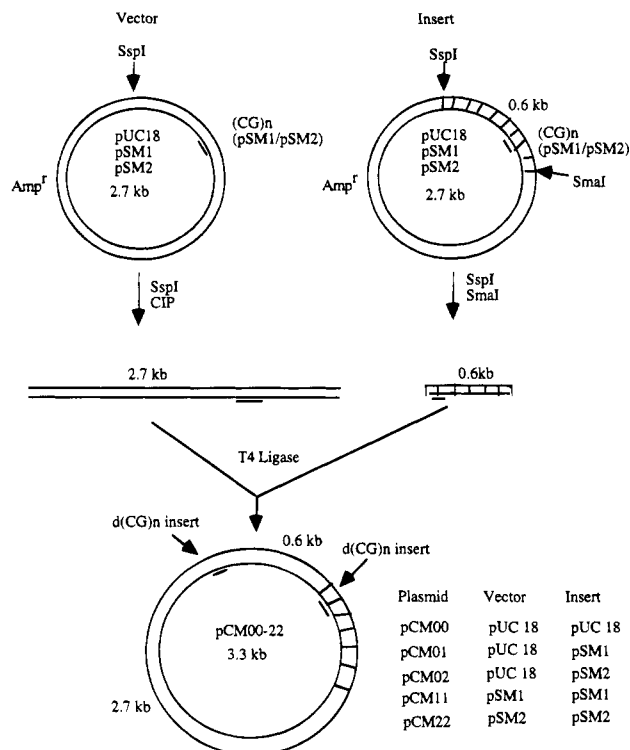


FIGURE 2: Schematic diagram of the process of construction of 3.3-kb plasmids pCM00, pCM01, pCM02, pCM11, and pCM22, which contain zero, one, or two d(CG)_n inserts.

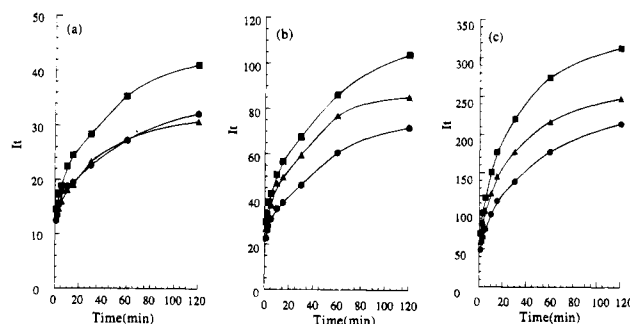


FIGURE 3: Relative total scattering intensity at 90° from plasmid DNA as a function of time after addition of condensing agent at different concentrations of Co(NH₃)₆³⁺: (a) 30 μM; (b) 50 μM; (c) 80 μM. (●) pUC18; (▲) pSM1; (■) pSM2. All solutions contained 5 μg/mL DNA, 1 mM sodium cacodylate, and 1 mM NaCl, pH 7.8. Experiments were done at room temperature, about 25 °C.

Circular pUC18, containing 2686 bp, was restricted at positions 411 and 417 by single-site restriction endonucleases *Pst*I and *Acc*I, respectively. Insert oligonucleotides containing 12-bp and 20-bp alternating d(CG)_n were synthesized by OLIGO Etc. (Ridgefield, CT). Figure 1 shows how the d(CG)_n sequence was cloned into pUC18. Proper insertion was confirmed by *Bss*III digestion and DNA sequencing using purified plasmids. The recombinant plasmids containing 12- and 20-bp inserts are denoted pSM1 and pSM2, respectively.

Plasmid Preparation. *Escherichia coli* DH5α containing pUC18, pSM1 or pSM2 was grown overnight in Luria–Bertani (LB) medium containing ampicillin. The plasmids were isolated by standard methods (Sambrook *et al.*, 1989) and purified by ethidium bromide–CsCl density gradient ultracentrifugation. Linear pUC18 (pUC18-1) was obtained by cutting with the single-site restriction endonuclease *Sca*I

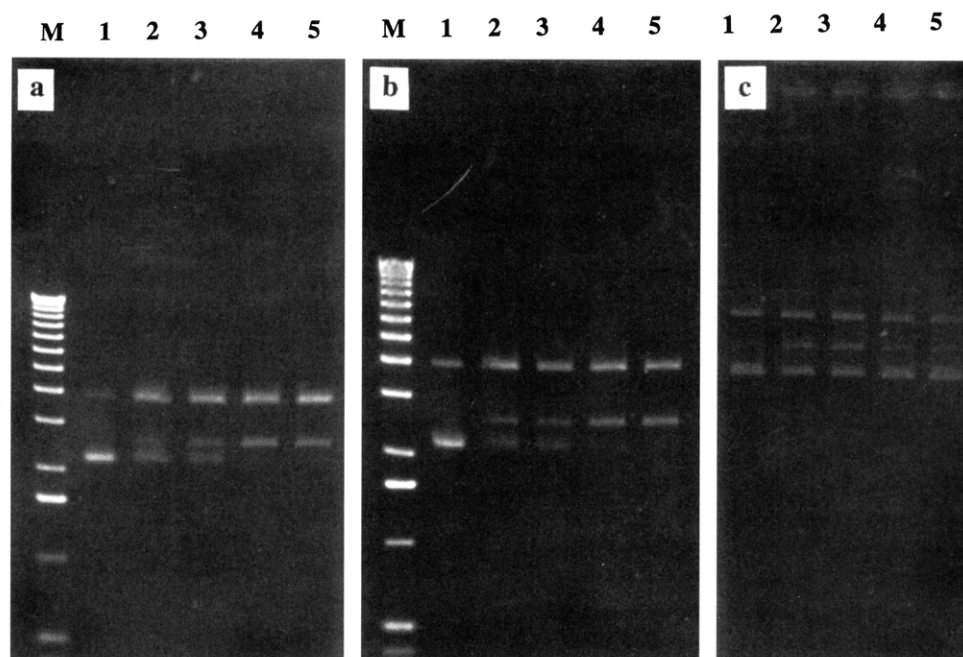


FIGURE 4: S1 nuclease digestion of plasmids (a) pSM1, (b) pSM2, and (c) pUC18 as a function of $\text{Co}(\text{NH}_3)_6^{3+}$ concentration. In each panel, lane M is a 1-kb ladder from Gibco-BRL; lanes 1–5 correspond to digested plasmid with $[\text{Co}(\text{NH}_3)_6^{3+}] = 0, 15, 30, 50,$ and $80 \mu\text{M}$, respectively. The order of increasing mobility is relaxed circular < linear < supercoiled molecules.

or *Bsr*F1 followed by phenol–chloroform extraction and ethanol precipitation. Stock DNA solutions of $50 \mu\text{g}/\text{mL}$ (determined by A_{260}) were made in 10 mM Tris-HCl/1 mM EDTA, pH 8.

Construction of Plasmids Containing Two $d(\text{CG})_n$ Inserts. Plasmids pCM00, pCM01, pCM02, pCM11, and pCM22, 3.3 kb long and containing zero, one, or two discrete $d(\text{CG})_n$ inserts were constructed by subcloning $d(\text{CG})_n$ -containing fragments from the existing plasmids pUC18, pSM1, or pSM2 according to the diagram in Figure 2. The parental vectors were obtained by linearizing these plasmids with *Ssp*I. Further digestion with *Ssp*I and *Sma*I produced blunt-end restriction fragments about 0.6 kb in length. These were isolated by agarose gel electrophoresis and a Millipore 0.45- μm Ultrafree-MC filter unit. The products were ligated and the ligation mixture was used to transform *E. coli* DH5 α competent cells. Ten transformants were selected for each reaction, and small plasmid preparations were performed and analyzed by restriction endonuclease digestion. The correct plasmids were selected and used for large-scale preparations.

Generation of Plasmids with Different Superhelical Densities. Different superhelical densities were obtained according to the method described by Singleton and Wells (1982), by incubating natural supercoiled DNA with 2 units of calf thymus topoisomerase I and various amounts of ethidium bromide (0–10 $\mu\text{g}/\text{mL}$) in 50 mM Tris-HCl (pH 7.5), 50 mM KCl, 0.1 mM EDTA, 0.5 mM dithiothreitol (DTT), and 30 $\mu\text{g}/\text{mL}$ bovine serum albumin (BSA) at 37 °C for 2 h. The reaction was stopped by phenol–chloroform extraction followed by ethanol precipitation, and then the DNA pellets were resuspended in 10 mM Tris-HCl (pH 8.0)/1 mM EDTA.

Chemical Modification of DNA with DEPC. DNA (1 μg) was diluted into 200 μL of solution containing 1 mM sodium cacodylate (pH 8), 1 mM NaCl, and 80 μM $\text{Co}(\text{NH}_3)_6^{3+}$ and left at room temperature for 2 h. Then 3 μL of diethyl pyrocarbonate was added and the solution was incubated at 20 °C for 15 min. The sample was mixed once during

incubation. Twenty microliters of 5 M NaCl and 600 μL of ethanol were added, and the sample was vortexed briefly and centrifuged at 10000g for 10 min. The DNA pellet was redissolved in 0.5 M NaCl/10 mM Tris-HCl (pH 8.0)/1 mM EDTA and reprecipitated with ethanol. The pellet was suspended in 100 μL of 1 M piperidine and incubated at 95 °C for 5 min. The DNA sample was purified by precipitating twice with ethanol, washed once with 70% ethanol, lyophilized, and resuspended in 10 mM Tris-HCl (pH 8.0)/1 mM EDTA.

S1 Nuclease Susceptibility. Aliquots (34 μL) of DNA solutions at 5 $\mu\text{g}/\text{mL}$ containing various $\text{Co}(\text{NH}_3)_6^{3+}$ concentrations were incubated at room temperature for 2 h. S1 nuclease at 910 units/ μL was diluted with 1 \times reaction buffer (50 mM NaCl/20 mM sodium acetate/0.1 mM ZnCl_2) to 91 units/ μL immediately before reaction, and then 2 μL of diluted enzyme and 4 μL of 10 \times reaction buffer were added to each sample and incubated at 37 °C for 20 min. Samples were left on ice until gel electrophoresis.

BssHII Digestion. Aliquots (52 μL) of DNA solutions at 5 $\mu\text{g}/\text{mL}$ containing various amounts of $\text{Co}(\text{NH}_3)_6^{3+}$ were incubated at room temperature for 2 h. *Bss*HII restriction endonuclease at 4 units/ μL , which is specific for the sequence GCGCGC, was diluted with 1 \times NEB reaction buffer for *Bss*HII (100 mM NaCl/10 mM Bis-tris propane hydrochloride/10 mM MgCl_2 /1 mM dithiothreitol) to 0.6 unit/ μL immediately before reaction, and then 6 μL of 10 \times reaction buffer and 2 μL of diluted enzyme were added to each sample and incubated at 37 °C for 15 min. Samples were left on ice until gel electrophoresis, for which 18- μL aliquots were used.

Light Scattering. Total intensity light scattering experiments were performed at 90° scattering angle with a Lexel argon-ion laser operating at 488 nm. Buffers were passed through 0.22- μm GS Millipore filters before mixing. Glassware was extensively rinsed with double-distilled water and baked before use. DNA stock solutions were passed through

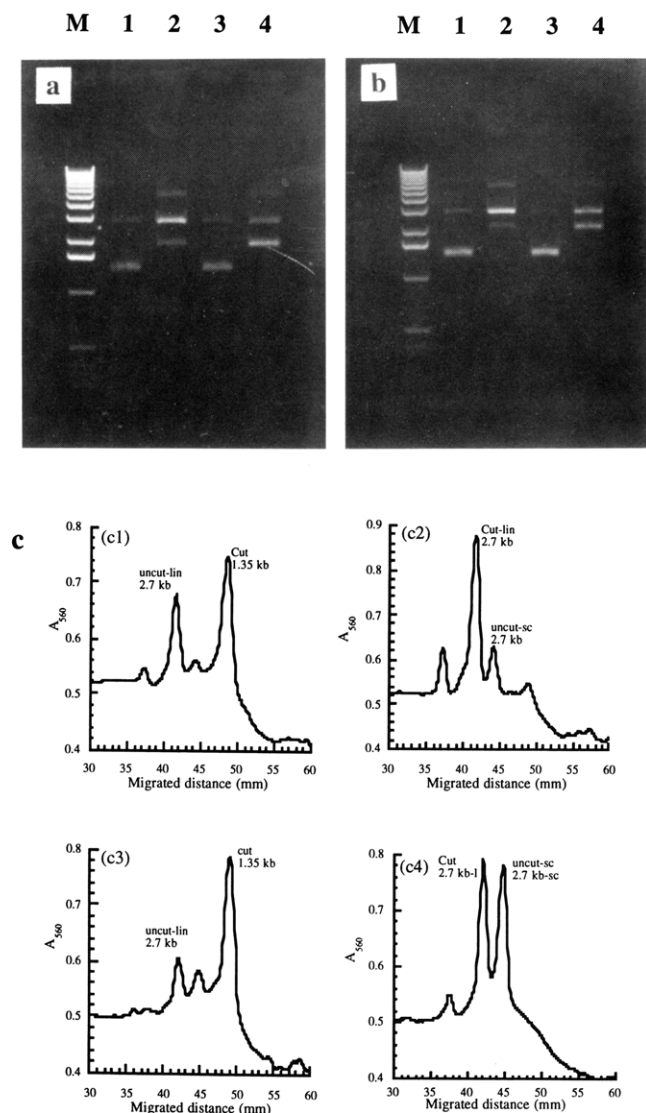


FIGURE 5: *Bss*HII digestion of linear (resulting from *Bsr*FI digestion) and supercoiled plasmids (a) pSM1 and (b) pSM2 with indicated concentrations of $\text{Co}(\text{NH}_3)_6^{3+}$. In each panel, lane M is a 1-kb ladder; lane 1, linear, 30 μM ; lane 2, supercoiled, 30 μM ; lane 3, linear, 80 μM ; lane 4, supercoiled, 80 μM . (c) Densitometric scan of panel b, with (c1–c4) corresponding to lanes 1–4.

0.45- μM GS Millipore filters before the concentration was measured by A_{260} . Intensities I_t plotted in Figures 3, 7, and 9 were measured on a scale on which a benzene standard gave 30.5. They were the average of 2–5 measurements on the same sample. Typical standard deviations were the size of the data symbols.

Electron Microscopy. Electron microscopy was carried out as described previously (Arscott *et al.*, 1990). Negatives were optically projected at 6 \times enlargement, and the images of individual particles were traced on paper, scanned, and measured with a digitizing program written in HyperCard on a Macintosh computer. For each toroid, the inner and outer radii were the average of two perpendicular measurements.

RESULTS

We used the large increase in light scattering intensity to monitor the condensation process. All condensation experiments were carried out at 5 $\mu\text{g}/\text{mL}$ DNA in a 1 mM sodium cacodylate/1 mM NaCl buffer, pH 7.8 at room temperature (about 25 $^\circ\text{C}$). Figure 3 shows the condensation kinetics of

pSM1 and pSM2 compared with the control pUC18 at $\text{Co}(\text{NH}_3)_6^{3+}$ concentrations of 30, 50 and 80 μM (panels a, b, and c). The plasmids with inserts condensed more rapidly and with a larger increase of scattering intensity, in the order of pSM2 > pSM1 > pUC18. This indicates that the d(CG)_n insert facilitates DNA condensation, and the longer the insert the greater the effect. The increase in scattering intensity with concentration of $\text{Co}(\text{NH}_3)_6^{3+}$, shown in the three panels of Figure 2, indicates that the extent of condensation increases (probably both more condensed particles and more DNA molecules per particle) as more condensing agent is added.

Since d(CG)_n inserts in supercoiled plasmids have been shown to convert to Z-form under physiological ionic conditions or in the presence of small amount of $\text{Co}(\text{NH}_3)_6^{3+}$, we wanted to ascertain whether the B to Z transition takes place under our experimental conditions. DNA molecules which contain d(CG)_n inserts show an increased susceptibility to S1 nuclease (Kim *et al.*, 1993); the nuclease is active at B–Z junctions (Peck *et al.*, 1982). Figure 4 shows the results of treating pSM1 and pSM2 with S1 nuclease after incubation with increasing concentrations of $\text{Co}(\text{NH}_3)_6^{3+}$. The pSM1 and pSM2 supercoils are nicked and cleaved more extensively within the 20-min incubation period as the $\text{Co}(\text{NH}_3)_6^{3+}$ concentration increases, which suggests either that the B to Z transition occurs more extensively or that other secondary structure perturbations are induced at higher $\text{Co}(\text{NH}_3)_6^{3+}$ concentrations. By contrast, the wild-type pUC18 control, when subjected to identical treatment, is only slightly converted to linear molecules, and the amount of cleavage remains invariant as the $\text{Co}(\text{NH}_3)_6^{3+}$ concentration increases. This shows that $\text{Co}(\text{NH}_3)_6^{3+}$ is not activating the S1 nuclease.

Restriction endonucleases are very sensitive to changes in conformation of both recognition and flanking sequences (Azorin *et al.*, 1984; Lesnik *et al.*, 1991; Singleton *et al.*, 1983). *Bss*HII has maximum reactivity for the B-conformation of GCGCGC (Azorin *et al.*, 1984). Therefore, the adoption of the Z conformation by d(GC)_n inserts can be assayed by measuring the inhibition of cleavage with *Bss*HII. Figure 5 shows the results of an experiment designed to measure the extent to which cleavage by *Bss*HII is inhibited in the supercoiled plasmids compared with the linear DNA. The d(CG)_n inserts, located at 0.42 kb, should remain in the B form in the linear molecules produced by cleavage of supercoiled pSM1 and pSM2 with *Bsr*FI at 1.78 kb. As seen in Figure 5, linear and supercoiled molecules were rapidly cleaved into 1.35-kb fragments and linear full-length molecules, respectively, by *Bss*HII at 30 μM $\text{Co}(\text{NH}_3)_6^{3+}$. However, at 80 μM $\text{Co}(\text{NH}_3)_6^{3+}$ the negatively supercoiled plasmids were less rapidly linearized, as shown by the persistence of supercoiled molecules. The densitometric scans of the pSM2 gel in Figure 5c make these conclusions more quantitative.

Diethyl pyrocarbonate (DEPC) reacts with purines in Z-DNA (Herr, 1985; Johnston, 1985, 1988; Kohwi-Shigematsu *et al.*, 1983) and B–Z junctions (Kohwi-Shigematsu *et al.*, 1987), modifying the N-6 and N-7 positions of adenine and the N-7 position of guanine when these sites are accessible. We therefore used DEPC to assay for Z-DNA structure in our plasmids. We condensed pUC18, pSM1, and pSM2 with 80 μM $\text{Co}(\text{NH}_3)_6^{3+}$, reacted it with DEPC, and then treated with piperidine, which cleaves DNA at the DEPC modification sites. As shown in Figure 6b, the

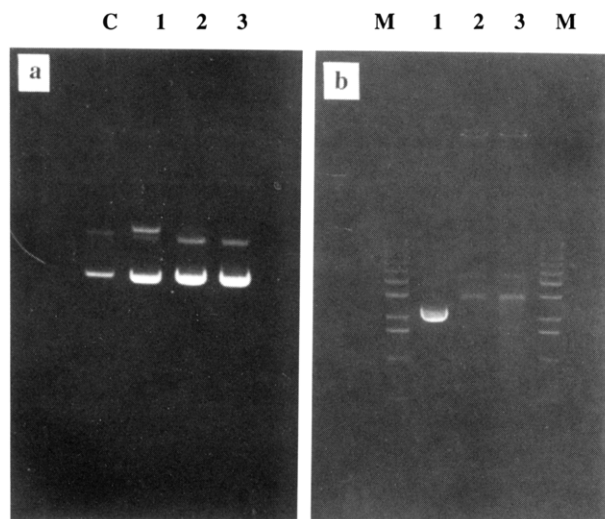


FIGURE 6: Gel electrophoresis of plasmids after diethyl pyrocarbonate modification and piperidine cleavage in the presence of (a) 30 μM and (b) 80 μM $\text{Co}(\text{NH}_3)_6^{3+}$. Lanes M, 1-kb ladder; lane C, pSM1 without treatment; lane 1, pUC18; lane 2, pSM1; lane 3, pSM2.

supercoiled forms of both pSM1 and pSM2 were cleaved to linear forms running at 2.7 kb, while the control pUC18 remained unchanged. This indicates that DEPC reacts with the $\text{d}(\text{CG})_n$ sequences and demonstrates that the inserts have converted to Z-form. These gels also show that the relaxed forms of pSM1 and pSM2 remain unmodified, confirming that $\text{d}(\text{CG})_n$ does not convert to Z-form without supercoiling. However, at 30 μM $\text{Co}(\text{NH}_3)_6^{3+}$, only small proportions of pSM1 and pSM2 were cleaved to the linear form, most remaining supercoiled as seen in Figure 6a. This suggests that, at $\text{Co}(\text{NH}_3)_6^{3+}$ concentrations near the condensation threshold, the inserts stay mainly in the B-form.

The foregoing experiments have demonstrated that $\text{d}(\text{CG})_n$ inserts in naturally supercoiled plasmids are able to flip from right-handed B-form to left-handed Z-form under our experimental conditions. The B–Z transition causes a reduction of superhelical density. In order to test whether the enhanced condensation of $\text{d}(\text{CG})_n$ -containing plasmids results from the change of superhelical density, control plasmid pUC18 was treated with topoisomerase I and increasing amounts of ethidium bromide which produced various degrees of supercoiling from totally relaxed to highly supercoiled ($\sigma = -0.14$ compared with -0.05 assumed for native plasmids). The resultant DNAs were incubated with 10–80 μM $\text{Co}(\text{NH}_3)_6^{3+}$ for 2 h at room temperature before the total scattering intensity was measured. Figure 7 shows that condensation of pUC18 without inserts is not affected by the superhelical density, which implies that the enhanced condensation of plasmids containing Z-DNA-forming sequences is not due to the superhelical density change while converting to Z-DNA.

Another possible cause of enhanced condensation is the $\text{d}(\text{CG})_n$ sequence itself, no matter what conformation it is in. This was tested by linearizing both insert and control plasmids by the single-site restriction endonuclease *ScaI*. All three plasmids should remain in B-form without topological constraints under our experimental conditions. Light scattering condensation curves (data not shown) are superimposable upon each other within experimental error, implying that the $\text{d}(\text{CG})_n$ insert does not affect DNA condensation when it is in the B-conformation.

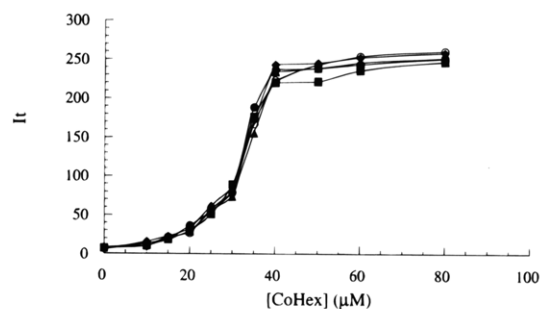


FIGURE 7: Scattering intensity of pUC18 plasmids 2 h after addition of $\text{Co}(\text{NH}_3)_6^{3+}$ as a function of condensing agent concentration and superhelical density. Solution conditions were 5 $\mu\text{g}/\text{mL}$ DNA, 1 mM NaCl, and 1 mM sodium cacodylate, pH 7.8. Ethidium bromide concentrations (micrograms per milliliter) and corresponding superhelical densities σ were (●) 0, 0; (■) 2.5, -0.04 ; (◆) 5.0, -0.08 ; (▲) 7.5, -0.11 ; (○) 10, -0.14 .

Table 1: Comparison of the Morphological Distributions for Control Plasmid pUC18 and $\text{d}(\text{CG})_n$ Insert Plasmids pSM1 and pSM2 in the Presence of Different Amounts of $\text{Co}(\text{NH}_3)_6^{3+}$

plasmid	$[\text{Co}(\text{NH}_3)_6^{3+}]$ (μM)	no. of toroids	toroid %	no. of rods	rod %
pUC18	30	159	91.9	14	8.1
	32	218	92.0	19	8.0
	40	166	97.6	4	2.4
pSM1	30	156	73.6	56	26.4
	32	155	89.6	18	10.4
	40	147	94.2	9	5.8
pSM2	30	107	78.1	30	21.9
	32	129	90.2	14	9.8
	40	85	96.6	3	3.4

Table 2: Inner and Outer Radii and Molecularity of Toroids for pUC18, pSM1, and pSM2 in the Presence of Different Amounts of $\text{Co}(\text{NH}_3)_6^{3+}$

plasmid	$[\text{Co}(\text{NH}_3)_6^{3+}]$ (μM)	R_{inner} (\AA)	R_{outer} (\AA)	molecularity
pUC18	30	124 ± 25	278 ± 24	4.0 ± 1.6
	32	133 ± 24	305 ± 34	5.6 ± 2.0
	40	121 ± 18	282 ± 18	4.5 ± 1.3
pSM1	30	130 ± 22	291 ± 28	4.8 ± 2.1
	32	75 ± 16	255 ± 35	4.7 ± 2.1
	40	86 ± 12	281 ± 31	6.0 ± 2.2
pSM2	30	122 ± 20	285 ± 31	4.6 ± 1.6
	32	72 ± 17	259 ± 28	5.0 ± 1.8
	40	78 ± 29	307 ± 36	8.7 ± 3.8

We used electron microscopy to investigate whether the condensed particles produced from wild-type and insert-containing plasmids had different morphologies. Samples were prepared 2 h after addition of 30–40 μM of $\text{Co}(\text{NH}_3)_6^{3+}$. Consistent with previous observations (Arscott *et al.*, 1990), the great majority of structures formed with pUC18 are toroids, regardless of $\text{Co}(\text{NH}_3)_6^{3+}$ concentration. However, as Table 1 shows, significant percentages of rods are observed with pSM1 and pSM2 at 30 μM $\text{Co}(\text{NH}_3)_6^{3+}$; the proportion of rods decreases at higher concentrations of condensing agent. In addition, the inner radii of the toroids formed with pSM1 and pSM2 decrease significantly as the $\text{Co}(\text{NH}_3)_6^{3+}$ concentration increases, while the outer radius remains roughly unchanged (see Table 2 and Figure 8). The molecularity, or average number of DNA molecules per toroid, calculated according to the procedure described in Arscott *et al.* (1990), increases as a result of the decrease of

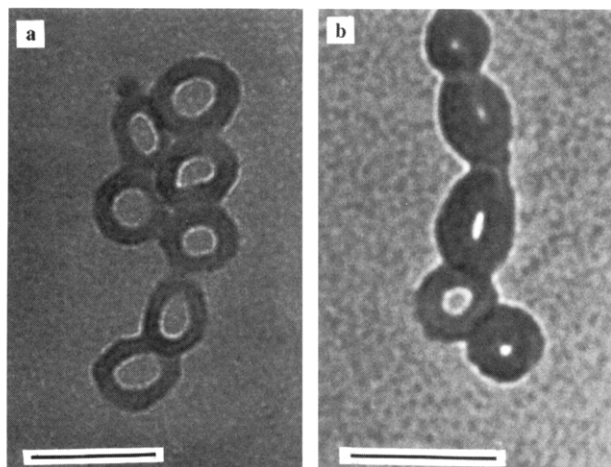


FIGURE 8: Electron micrographs of (a) pUC18 and (b) pSM2 after addition of $32 \mu\text{M Co}(\text{NH}_3)_6^{3+}$. The bars represent 1000 \AA .

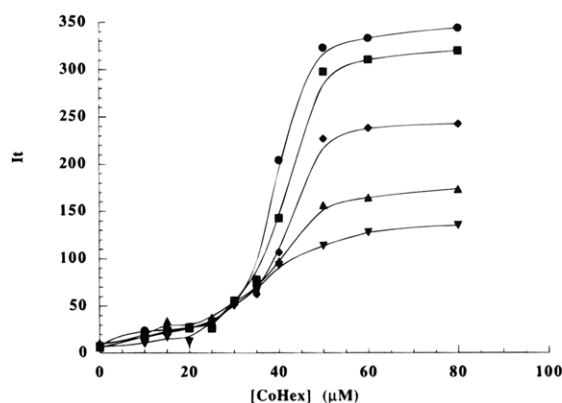


FIGURE 9: Scattering intensity 2 h after addition of $\text{Co}(\text{NH}_3)_6^{3+}$ as a function of condensing agent concentration. (∇) pCM00; (\blacktriangle) pCM01; (\blacklozenge) pCM02; (\blacksquare) pCM11; (\bullet) pCM22.

inner radius. This presumably accounts for at least part of the higher light scattering intensity observed in Figure 3.

Matters become more complicated if two separated $\text{d}(\text{CG})_n$ inserts are present in the same supercoiled plasmid, since they must compete for the limited free energy of supercoiling. It has been demonstrated that the B–Z transition of one small insert in supercoiled DNA can affect the conformational transition of another insert at a distance within the same topological domain (Ellison *et al.*, 1987; Kelleher *et al.*, 1986). We extended our analysis of the connection between condensation and the B–Z transition to plasmids with natural superhelical density containing two $\text{d}(\text{CG})_n$ sequences separated by 0.6 kb, prepared as diagrammed in Figure 2. Figure 9 shows the light scattering intensity as a function of $\text{Co}(\text{NH}_3)_6^{3+}$ concentration 2 h after condensation. At $40 \mu\text{M}$ or higher $\text{Co}(\text{NH}_3)_6^{3+}$, the intensity increases as the length of the insert increases, in the order $\text{pCM22} > \text{pCM11} > \text{pCM02} > \text{pCM01} > \text{pCM00}$. This is consistent with the behavior plotted in Figure 3, showing that DNA with longer inserts condenses more extensively.

In order to test whether both $\text{d}(\text{CG})_n$ inserts convert from B- to Z-form, DEPC chemical probing and piperidine cleavage was carried out for pCM22 in the presence of $80 \mu\text{M Co}(\text{NH}_3)_6^{3+}$. Figure 10 shows that the majority of the supercoiled pCM22 is cleaved into 2.7-kb and 0.6-kb fragments, consistent with the conversion of both inserts. There is, however, a light band corresponding to the linear 3.3-kb form of pCM22, implying that in a small fraction of

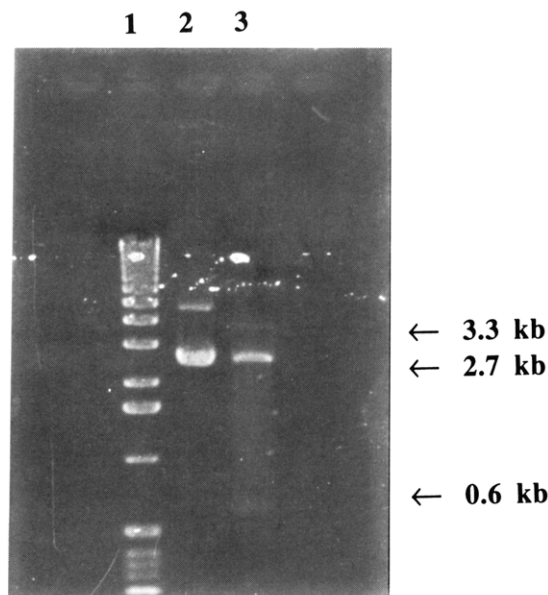


FIGURE 10: Gel electrophoresis of pCM22 after diethyl pyrocarbonate modification and piperidine cleavage in the presence of $80 \mu\text{M Co}(\text{NH}_3)_6^{3+}$. Lane 1, 1-kb ladder; lane 2, pCM22 without any treatment; lane 3, pCM22 + DEPC + piperidine.

pCM22 only one $\text{d}(\text{CG})_n$ insert converts to Z-form.

DISCUSSION

We have shown that $\text{Co}(\text{NH}_3)_6^{3+}$ can induce a B–Z conformational transition in sequences of $\text{d}(\text{CG})_6$ and $\text{d}(\text{CG})_{10}$ inserted into pUC18 plasmid DNA and that the B–Z transition enhances DNA condensation. The B–Z transition is detectable at $30 \mu\text{M Co}(\text{NH}_3)_6^{3+}$, near the onset of condensation, but it is more advanced at higher $\text{Co}(\text{NH}_3)_6^{3+}$ concentrations. Future work should delineate more precisely the range over which most of the B–Z transition occurs. Control experiments with the parental plasmid demonstrate that the B–Z transition is a property of the $\text{d}(\text{CG})_n$ insert and that it is facilitated by the torsional stress of negative supercoiling.

The connection between the Z-conformation and DNA condensation is consistent with previous reports. The Z-conformation of $\text{d}(\text{CG})_n$ has a strong tendency to aggregate in solutions containing metal cations or alcohols (Van de Sande & Jovin, 1982; Van de Sande *et al.*, 1982; Zacharias *et al.*, 1983). Z-DNA aggregates into well-ordered fibrous structures (Chaires & Norcum, 1988) in the presence of divalent cations and under various solvent conditions; this form is called Z*-DNA (Van de Sande & Jovin, 1982). A toroidal condensed form of left-handed poly(dG-m⁵dC) was observed in the presence of $5 \mu\text{M Co}(\text{NH}_3)_6^{3+}$ (Thomas & Bloomfield, 1985); similar structures form in poly(dG-m⁵dC) solutions containing only NaCl.

Our experiments were done at very low ionic strengths, about 1.5 mM Na^+ , which is similar to the conditions under which numerous other DNA condensation studies have been performed. At this ionic strength, the $\text{Co}(\text{NH}_3)_6^{3+}$ concentration at the midpoint of the condensation transition is in the range $30\text{--}40 \mu\text{M}$ for the various plasmids (Figures 7 and 9). It is interesting to compare this with the midpoints of the B–Z flipping transitions provoked by trivalent cations at higher ionic strengths that are closer to physiological. Peck *et al.* (1982) found the midpoint near $100 \mu\text{M Co}(\text{NH}_3)_6^{3+}$ for plasmids with $\text{d}(\text{C-G})$ inserts in 100 mM ionic strength

buffers. Thomas *et al.* (1991), also using plasmids with GC inserts, found a midpoint of 280 μ M spermidine in a 50 mM NaCl buffer with 1 mM sodium cacodylate and 0.15 mM EDTA, pH 7.4. These results are consistent with previous observations of the increased concentration of trivalent ion needed for competition with monovalent cation (Wilson & Bloomfield, 1979) and the greater effectiveness of $\text{Co}(\text{NH}_3)_6^{3+}$ relative to spermidine (Widom & Baldwin, 1980). Interestingly, for plasmids containing $(\text{dA-dC})_n(\text{dG-dT})_n$ inserts in 50 mM NaCl buffer, the concentration of spermidine needed for the midpoint of the B-Z transition is only 25 μ M and $\text{Co}(\text{NH}_3)_6^{3+}$ had no effect (Thomas & Thomas, 1994). This indicates a specific interaction dependent on polyamine structure.

What is surprising about our results is that such short segments of Z-DNA can facilitate condensation of molecules that are almost entirely B-DNA. The $\text{d}(\text{CG})_n$ inserts are only 0.45% and 0.74% of the total length of DNA in pSM1 and pSM2, respectively, but they have a large effect on the compactness and morphology of the condensed DNA. It may be either that the inserts serve as local nuclei or that they have longer-range structural effects. Unfortunately, we have no evidence that distinguishes between these mechanisms. The latter is consistent with the striking observation (Kim *et al.*, 1993) that a 16-base-pair $\text{d}(\text{CG})_8$ sequence in a 1.1-kb restriction fragment of pBR322 has a long-range effect, extending over 330–550 bp, on the dynamical secondary structure of the (linear) fragment. The potential coupling of short- and long-range effects is even more credible, of course, in closed circular molecules.

A local nucleation role for Z-DNA may be related to the properties of Z-DNA itself or the B-Z junction or both. Crystallography of the Z-form of alternating $\text{d}(\text{CG})$ oligonucleotides shows the formation of a large uncharged surface (Wang *et al.*, 1979; Arnott *et al.*, 1980; Drew *et al.*, 1980). Haniford & Pulleyblank (1983) have suggested that this may reduce electrostatic repulsions and allow the close approach of these segments in the plasmid. Electron microscopy shows a higher proportion of rods at 30 μ M $\text{Co}(\text{NH}_3)_6^{3+}$ for pSM1 and pSM2 than for pUC18 and smaller inner radii of toroids at higher concentrations of condensing agent. This suggests that B-Z junctions produce kinking or flexibility that facilitates the tight curvature needed for such structures. The S1 nuclease susceptibility results shown in Figure 4 imply that more secondary structure perturbations appear in plasmids containing $\text{d}(\text{CG})_n$ inserts as the $\text{Co}(\text{NH}_3)_6^{3+}$ concentration increases. Several lines of evidence, including enzymatic and chemical reactivity and electrophoretic mobility, suggest that B-Z junctions increase the bending and/or flexibility of DNA (Johnston, 1985, 1988; Klysik *et al.*, 1983; Lu *et al.*, 1992; Palecek *et al.*, 1987; Winkle *et al.*, 1991).

Finally, since pCM11 with two 12-bp inserts has a significantly higher scattering intensity than pCM02 with a single 20-bp insert (Figure 9), there is a hint that two separated short inserts can initiate condensation more effectively than a single long one, either by providing two nucleation centers or by coming together to form an intraring complex.

REFERENCES

- Arnott, S., Chandrasekaran, R., Birdsall, D. L., Leslie, A. G. W., & Ratliff, R. L. (1980) *Nature* 283, 743–745.
- Arcott, P. G., Li, A.-Z., & Bloomfield, V. A. (1990) *Biopolymers* 30, 619–630.
- Azorin, F., Hahn, R., & Rich, A. (1984) *Proc. Natl. Acad. Sci. U.S.A.* 81, 5714–5718.
- Behe, M., & Felsenfeld, G. (1981) *Proc. Natl. Acad. Sci. U.S.A.* 78, 1619–1623.
- Castleman, H., & Erlanger, B. F. (1983) *Cold Spring Harbor Symp. Quant. Biol.* 47, 133–142.
- Chaires, J. B., & Norcum, M. T. (1988) *J. Biomol. Struct. Dyn.* 5, 1187–1207.
- Chattoraj, D. K., Gosule, L. C., & Schellman, J. A. (1978) *J. Mol. Biol.* 121, 327–337.
- Drew, H., Takano, T., Tanaka, S., Itakura, K., & Dickerson, R. E. (1980) *Nature* 286, 567–573.
- Ellison, M. J., Fenton, J., Ho, P. S., & Rich, A. (1987) *EMBO J.* 6, 1513–1522.
- Gosule, L. C., & Schellman, J. A. (1976) *Nature* 259, 333–335.
- Haniford, D. B., & Pulleyblank, D. E. (1983) *J. Biomol. Struct. Dyn.* 1, 593–609.
- Herr, W. (1985) *Proc. Natl. Acad. Sci. U.S.A.* 82, 8009–8013.
- Johnston, B. H. (1985) *Cell* 42, 713–724.
- Johnston, B. H. (1988) *J. Biomol. Struct. Dyn.* 6, 153–166.
- Kelleher, R. J., III, Ellison, M. J., Ho, P. S., & Rich, A. (1986) *Proc. Natl. Acad. Sci. U.S.A.* 83, 6342–6346.
- Kim, U.-S., Fujimoto, B. S., Furlong, C. E., Sundstrom, J. A., Humbert, R., Teller, D. C., & Schurr, J. M. (1993) *Biopolymers* 33, 1725–1745.
- Klysik, J., Stirdivant, S. M., Singleton, C. K., Zacharias, W., & Wells, R. D. (1983) *J. Mol. Biol.* 168, 51–71.
- Kohwi-Shigematsu, T., Gelinas, R., & Weintraub, H. (1983) *Proc. Natl. Acad. Sci. U.S.A.* 80, 4389–4393.
- Kohwi-Shigematsu, T., Manes, T., & Kohwi, Y. (1987) *Proc. Natl. Acad. Sci. U.S.A.* 84, 2223–2227.
- Lesnik, E. A., Bes'chetnikova, Z. A., Maslova, R. N., & Varshavsky, J. M. (1991) *FEBS Lett.* 280, 91–93.
- Lu, M., Guo, Q., Kallenbach, N. R., & Sheardy, R. D. (1992) *Biochemistry* 31, 4712–4719.
- Manning, G. S. (1978) *Q. Rev. Biophys.* 11, 179–246.
- Manning, G. S. (1980) *Biopolymers* 19, 37–59.
- Manning, G. S. (1981) *Biopolymers* 20, 1261–1270.
- Marquet, R., & Houssier, C. (1991) *J. Biomol. Struct. Dyn.* 9, 159–167.
- Marquet, R., Houssier, C., & Fredericq, E. (1985) *Biochim. Biophys. Acta* 825, 365–374.
- Oosawa, F. (1971) *Polyelectrolytes*, Marcel Dekker, New York.
- Palecek, E., Boubliková, P., Nejedlý, K., Galazka, G., & Klysik, J. (1987) *J. Biomol. Struct. Dyn.* 5, 297–306.
- Peck, L. J., Nordheim, A., Rich, A., & Wang, J. C. (1982) *Proc. Natl. Acad. Sci. U.S.A.* 79, 4560–4564.
- Plum, G. E., Arcott, P. G., & Bloomfield, V. A. (1990) *Biopolymers* 30, 631–643.
- Porschke, D. (1984) *Biochemistry* 23, 4821–4828.
- Rau, D. C., & Parsegian, V. A. (1984) *Biophys. J.* 45, 114a.
- Rau, D. C., & Parsegian, V. A. (1992) *Biophys. J.* 61, 260–271.
- Rau, D. C., Lee, B. K., & Parsegian, V. A. (1984) *Proc. Natl. Acad. Sci. U.S.A.* 81, 2621–2625.
- Revet, B., Delain, E., Dante, R., & Niveleau, A. (1983) *J. Biomol. Struct. Dyn.* 1, 857–871.
- Riemer, S. C., & Bloomfield, V. A. (1978) *Biopolymers* 17, 785–794.
- Sambrook, J., Fritsch, E. F., & Maniatis, T. (1989) *Molecular Cloning: A Laboratory Manual*, Cold Spring Harbor Press, Cold Spring Harbor, NY.
- Schellman, J. A., & Parthasarathy, N. (1984) *J. Mol. Biol.* 175, 313–329.
- Singleton, C. K., & Wells, R. D. (1982) *Anal. Biochem.* 122, 253–257.
- Singleton, C. K., Klysik, J., Stirdivant, S. M., & Wells, R. T. (1982) *Nature* 299, 312–316.
- Singleton, C. K., Klysik, J., & Wells, R. D. (1983) *Proc. Natl. Acad. Sci. U.S.A.* 80, 2447–2451.
- Thomas, T. J., & Bloomfield, V. A. (1985) *Biochemistry* 24, 713–719.
- Thomas, T. J., & Thomas, T. (1994) *Biochem. J.* 298, 485–491.
- Thomas, T. J., Gunnia, U. B., & Thomas, T. (1991) *J. Biol. Chem.* 266, 6137–6141.

- Van de Sande, J. H., & Jovin, T. M. (1982) *EMBO J.* 1, 115–120.
- Van de Sande, J. H., McIntosh, L. P., & Jovin, T. M. (1982) *EMBO J.* 1, 777–782.
- Wang, A. H.-J., Quigley, G. J., Kolpak, F. J., Crawford, J. L., van Boom, J. H., van der Marel, G., & Rich, A. (1979) *Nature* 282, 680–686.
- Widom, J., & Baldwin, R. L. (1980) *J. Mol. Biol.* 144, 431–453.
- Widom, J., & Baldwin, R. L. (1983) *Biopolymers* 22, 1595–1620.
- Wilson, R. W., & Bloomfield, V. A. (1979) *Biochemistry* 18, 2192–2196.
- Winkle, S. A., Aloyo, M. C., Morales, N., Zambrano, T. Y., & Sheardy, R. D. (1991) *Biochemistry* 30, 10601–10606.
- Zacharias, W., Martin, J. C., & Wells, R. D. (1983) *Biochemistry* 22, 2398–2405.

BI942249X